INVESTIGATION OF POINCARE SOLUTIONS OF NONLINEAR DUFFING AND PENDULUM UNDER SELECTED PERIODIC EXCITATIONS USING FRACTAL DISK CHARACTERISATION

ABSTRACT

Literature has shown that harmonically excited nonlinear Duffing and pendulum oscillators can respond chaotically under the influence of some of their drive parameters combination. However, literature is scarce on the steady state responses of these oscillators when excited arbitrarily and periodically. Therefore, this research was designed to investigate the potential qualitative and quantitative variation in the steady Poincare solutions of nonlinear Duffing and pendulum oscillators under selected periodic excitations compared to their harmonically excited counterparts. The non-dimensional second Order Differential Equation (ODE) corresponding respectively to governing equations for harmonically/periodically excited nonlinear Duffing and pendulum were solved using the constant step fourth order Runge-Kutta algorithms. The corresponding steady state Poincare solutions obtained were characterised by visual inspection and fractal dimension measure obtained using fractal disk counting method. Visual inspection of corresponding steady Poincare solutions show that they are qualitatively indistinguishable. However, the corresponding estimated fractal dimension varied significantly. The absolute variation in dimension was found to be between 1.37% and 4.92% for the Duffing oscillator and between 5.67% and 7.39% for the pendulum oscillator.

Keywords: *Excited Duffing Oscillator, Excited Pendulum Oscillator, Fourth-order Runge-Kutta, Fourier transformation, Periodic Excitation, Poincare section, and Fractal disk characterisation.*

1.0 INTRODUCTION

Nonlinearity is a term with broad applications in nature [1]. Systems in which the variation in the input does not give an equivalent change in the output are said to be nonlinear systems. Many natural systems behaviors do not follow a systematic pattern; thus, it requires an appropriate method to grasp the systems well. As a result of many systems being nonlinear in nature, nonlinear problems are encountered in many areas of science and engineering, such as fluid flow problem, chemical kinetics, structural dynamics and mechanical vibration [2]. The system is of interest to biologists, physicists, mathematicians, engineers, and many other scientists. The behavior of a nonlinear system in mathematics is expressed by a nonlinear system of equations. In recent times, new and abstract mathematical tools have emerged for solving nonlinear problems. Chaos in nonlinear oscillators of the Duffing type has attracted a lot of attention [3].

Nonlinear vibrations are a common occurrence in modern machinery because of the combination of higher operating speeds and lighter materials. Because many mechanical elements exhibit various sorts of nonlinearities, the scope of equations of motion expands dramatically; therefore, the mathematical model expressing the equation of motion can include several orders and an infinite number of possible coefficients. The most common models of nonlinear systems are a nonlinear pendulum, the Van der Pol and Duffing oscillators, self-excited vibrations, and friction [4][5]. Most of the parts that contribute to nonlinearities in mechanical systems, such as gears, bearings, and friction elements, are described by these models. Numerical approaches such as the Runge-Kutta method are used to find solutions [5].

The numerical approach [6] is crucial in solving nonlinear differential equations, according to a thorough examination of the literature. The most extensively used globally accepted numerical approaches are backward differential formulae, Runge-Kutta, and Adam-Bashforth-Moulton. The Runge-Kutta family of algorithms is still the most popular and widely used integration method [7]. The simplicity, stability, and self-starting character of Runge-Kutta procedures are their main features. The main disadvantages of Runge-Kutta procedures are that they take a lot more computer time than multi-step systems with comparable accuracy and that getting reasonable global estimates of the truncation error is challenging. However, for the simple dynamical systems discussed in this course, the relative simplicity and convenience of the use of Runge-Kutta methods far outweighs the drawback of their complexity.

Nonlinear oscillations are inextricably linked to the Duffing equation [8], often known as the Duffing oscillator. The Duffing oscillator is also thought to be a prototype for nonlinear dynamics systems. Many investigations on chaotic systems defined by a time-forced, dissipative, second-order nonlinear differential equation have used Duffing's equation as a model. Different words might be used, but the basic equation relates to a model for a long and narrow vibrating beam positioned between two permanent magnets and exposed to an external sinusoidal force [9].

Furthermore, from the first scientific investigation by Galileo in 1602, the regular motion of the pendulum was used for timekeeping, and it was the world's most accurate timekeeping technology until 1930. Galileo discovered the crucial property that makes the pendulum a crucial timekeeper called isochronisms; the pendulum's period is approximately independent of the amplitude or width of the swing. Through the seventeenth, eighteenth, nineteenth, and early twentieth centuries, the pendulum played an essential role in developing classical mechanics. Santori invented a device that measured a patient's pulse by the pendulum's length. By the mid-20th century, the invention of digital computers led to an exponential increase in studying the mechanics of the pendulum. Today its interest cuts across several fields, from science and engineering to education, military, civil, and industry, due to the broad range of applications [10].

Since Galileo's first observations of the pendulum system, many researchers and authors have likewise studied the pendulum and applied its theory and principles to problems of repetitive or vibratory motion. The angular displacement and its derivatives are the solutions to the governing equation of the pendulum. These solutions or the response of the pendulum could be periodic or otherwise. For a periodic response of the nonlinear pendulum, the solutions repeat at regular periods. [11] described the periodic response in their work, they stated that the pendulum's response when plotted could be such that the displacement repeats in time at regular intervals. However, they stated that other forms of response are possible. Such other responses are described as aperiodic, non-periodic responses and could be chaotic, quasi-periodic, or almost periodic [12]. A quasi-periodic response will appear to have more than one type of behavior that it repeats. For example, it may have more than one maximum amplitude value of displacement that it repeats.

The frequency response curve, backbone curve, and when using the numerical approach, time histories are the most common tools used in the analysis of nonlinear systems. However, more specialized techniques might be noted among the more complex tools: phase portraits, bifurcation diagrams, fractal dimension, basins of attraction and Poincaré maps, and Lyapunov exponent [13].

Fractals are mathematical objects that have the same pattern at all scales. They are usually manifolds that are not differentiable in any way. To characterize fractals, the concept of dimension must be expanded to include non-integer values. In contrast, fractal geometry accommodates all shapes present in the actual world, regardless of complexity, without attempting to force them to conform to any of the unnatural Euclidean shapes [14]. Trees, coastlines, cloud formations, leaf venations, fruit shapes, voice signals, and other real-world shapes are examples. In consequence, although Euclidean geometry has limitations in terms of analyzing complex and rough shapes, fractal geometry can handle any shape, regardless of complexity. A fractal is a rough or shattered geometric shape that may be broken into parts, each portion being a smaller version of the whole pattern. Self-similarity is a term used to describe this self-repeating phenomenon. A little fragment of a fractal item resembles a larger piece of the thing or the entire object when inspected. Because of their essential quality, fractals are widely used in computer modeling of irregular patterns and structures in nature [15]. This is because fractals are geometric

patterns that are repeated at lower and smaller scales to produce irregular shapes and surfaces that classical geometry cannot represent.

The Poincare Map is a tool for investigating periodic or nearly periodic orbits' asymptotic stability. Poincare's map constitutes a procedure employed to eliminate a dimension of the system and, therefore, a continuous system is transformed into a discrete one. It can also be considered as a surface that transversely intersects a given orbit [16].

Therefore, the Poincare section simplifies the visualization of a complex shape without tampering with its underlying dynamics [17]. Also, the Poincare section is similar to using a plane to cut through the trajectory of the fractal shape in phase space at regular intervals and make plot recordings of the points at which the fractal trajectory cuts the sectioning plan.

This article seeks to characterize the obtained steady-state Poincare solutions of both the periodically excited nonlinear pendulum and Duffing oscillator by visual examination and fractal dimension measurement using the fractal disk counting method.

2.0 METHODOLOGY

2.1 Duffing Equation

The present study adopted the already reduced duffing equation (1). It is expressed in dimensionless form to reduce the number of adjustable parameters [7].

$$\ddot{x} + \gamma\dot{x} - \frac{x}{2}(1 - x^2) = P_o \sin(\omega_D t) \qquad (1)$$

In equation (1), x, $\dot{x}$, $\ddot{x}$ represent displacement, velocity and acceleration of the oscillator about a datum point. Where 'γ' controls the amount of damping, P_o is the Amplitude strength of the harmonic excitation, ω_D is the excitation frequency, and t is the time [18].

2.2 Periodic Excitation of Duffing Oscillator using Fourier transformation

The harmonic function $P_o \sin(\omega_D t)$ is converted to periodic, generalizing the terms, using fourier transformation. The Fourier series representing the function can be expressed as

$$f(t) = P_0 + \sum_{n=1}^{\infty}(P_n \cos \omega_n t + b_n \sin \omega_n t) \qquad (2)$$

Where $P_0 = \frac{\omega}{\pi}\int_0^{\frac{2\pi}{\omega}} f(t)\ dt$ (3)

$P_n = \frac{\omega}{\pi}\int_0^{\frac{2\pi}{\omega}} f(t)\cos \omega_n t\ \ dt$ (4)

$Q_n = \frac{\omega}{\pi}\int_0^{\frac{2\pi}{\omega}} f(t)\sin \omega_n t\ \ dt$ (5)

In this research, two wave forms (periodic excitations) were considered.

2.2.1 Excitation

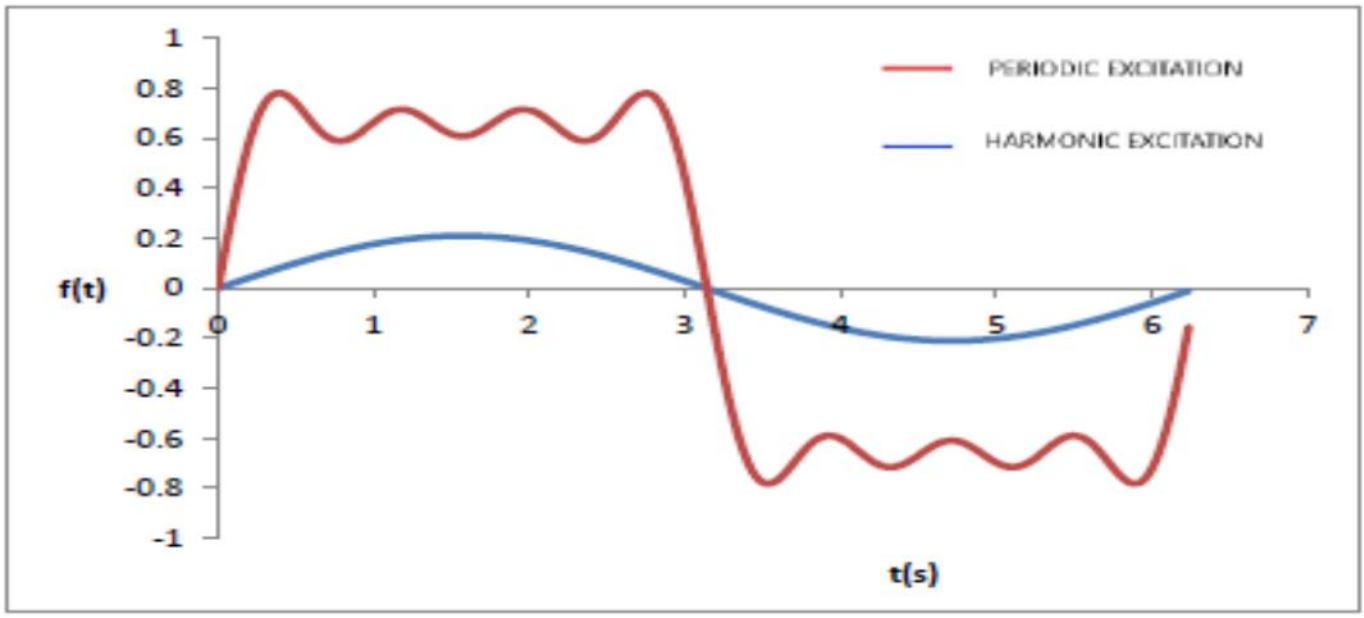

Fig 1. Periodic excitation 1 (square form) up to 7th term harmonics

Considering the periodic excitation 1, using fourier series, the forcing term required, yields,

$P_n = 0$

$Q_0 = 0$

$Q_n = 0$ (for all even n)

$Q_n = \frac{1}{n\pi}[1 - 2\cos(n\pi) + \cos(2n\pi)]$ (for all odd n) **(6)**

Rescaling the terms to have the same strength as the forcing amplitude,

$Q_n = \frac{Q_n}{Q_1} \times P_0$ (where P_0 is the Amplitude strength of the duffing oscillator)

$$f(t) = Q_1 \sin \omega_1 t + Q_3 \sin \omega_3 t + Q_5 \sin \omega_5 t + Q_7 \sin \omega_7 t \quad \textbf{(7)}$$

2.2.2 Excitation 2

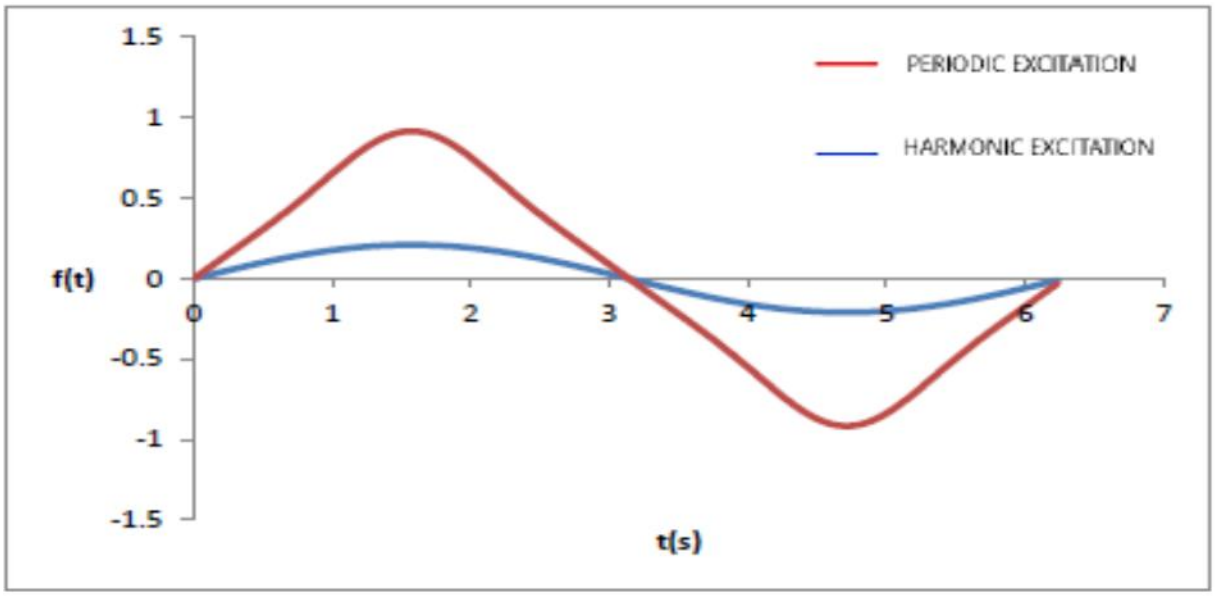

Fig 2. Periodic excitation 2 (triangular form) up to 7th term harmonics

Considering the periodic excitation 2, using Fourier series, the forcing term required yields,

$P_n = 0$

$Q_0 = 0$

$Q_n = 0$ (for all even n)

$Q_n = \frac{8}{(n\pi)^2} \sin\left(\frac{n\pi}{2}\right)$ (for all odd n) **(8)**

Rescaling the terms to have the same strength as the forcing amplitude,

$Q_n = \frac{Q_n}{Q_1} \times P_0$ (where P_0 is the Amplitude strength of the duffing oscillator).

The forcing term then is;

$$f(t) = Q_1 \sin \omega_1 t + Q_3 \sin \omega_3 t + Q_5 \sin \omega_5 t + Q_7 \sin \omega_7 t \quad \textbf{(9)}$$

2.3 Pendulum Equation

$$\frac{d^2\theta}{dt^2} + \frac{1}{q}\frac{d\theta}{dt} + \sin\theta = g\cos(\omega t) \quad \textbf{(10)}$$

It should be noted here that equation 10, is similar to the non-dimensional form of the forced nonlinear pendulum found in reviewed literature [11], with a natural oscillation frequency of unity applied. The number of adjustable parameters has been reduced to just three, that is the non-dimensional forcing amplitude (*g*), the non-dimensional damping factor (q) and the drive frequency (ω). Where $\theta, \frac{d\theta_1}{dt}, \frac{d^2\theta}{dt^2}$ are

respectively, the angular displacement, undifferentiated), (angular velocity, first order differential) and (angular acceleration, second order differential).

2.4 Periodic Excitation of pendulum using Fourier transformation

The harmonic function g *cos* (ωt) is converted to periodic, generalizing the terms, using Fourier transformation. The Fourier series representing the function can be expressed as

$$f(t) = P_0 + \sum_{n=1}^{\infty}(P_n \cos \omega_n t + b_n \sin \omega_n t) \qquad \textbf{(11)}$$

Where $P_0 = \frac{\omega}{\pi} \int_0^{\frac{2\pi}{\omega}} f(t) \quad dt$ **(12)**

$P_n = \frac{\omega}{\pi} \int_0^{\frac{2\pi}{\omega}} f(t) \cos \omega_n t \quad dt$ **(13)**

$Q_n = \frac{\omega}{\pi} \int_0^{\frac{2\pi}{\omega}} f(t) \sin \omega_n t \quad dt$ **(14)**

In this research, two wave forms (periodic excitations) were considered.

2.4.1 Excitation 3

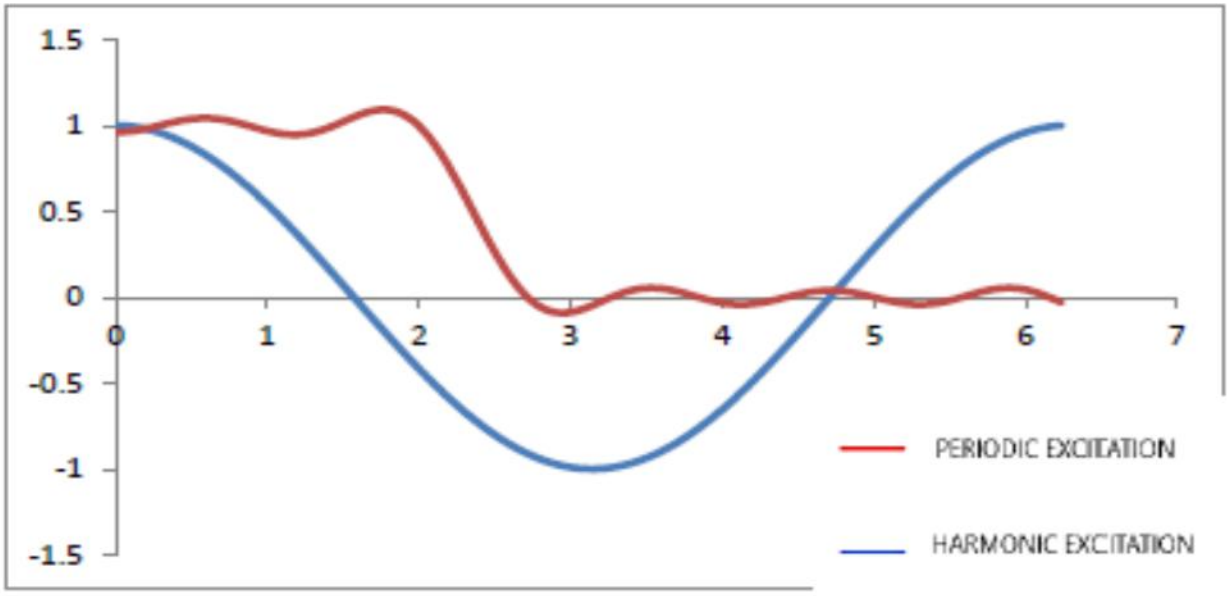

Fig 3. Periodic excitation 3 (square form) up to 7th term harmonics

Considering the periodic excitation 3, using Fourier series, the forcing term required yields,

$Q_n = 0$

$P_0 = 1/2$

$P_n = 0$ (for all even n)

$P_n=\frac{2}{n\pi}[-1]^{\frac{n-1}{2}}$ (for all odd n) **(15)**

Rescaling the terms to have the same strength as the forcing amplitude,

$P_n=\frac{P_n}{P_1}\times g$

$f(t)=\frac{1}{2}+P_1\cos\omega_1 t+P_3\cos\omega_3 t+P_5\cos\omega_5 t+P_7\cos\omega_7 t$ **(16)**

2.4.2 Excitation 4

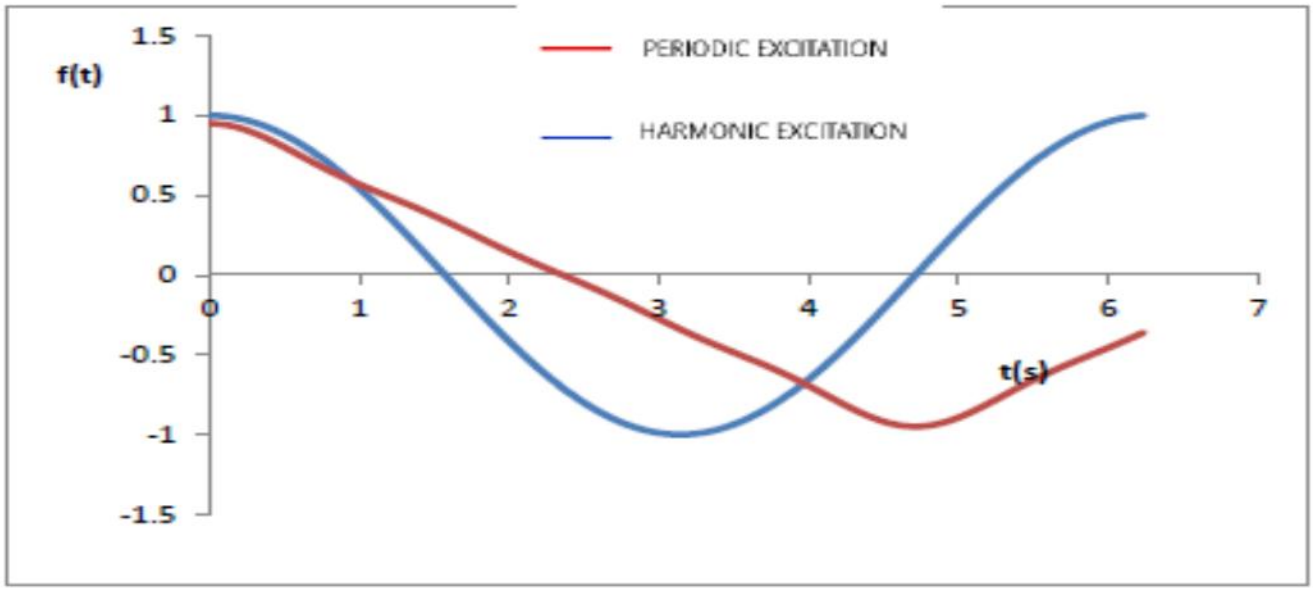

Fig 4. Periodic excitation (triangular form) up to 7th term harmonics

Considering the periodic excitation 4, using fourier series, the forcing term required yields,

$Q_n=0$

$P_0=0$

$P_n=0$ (for all even n)

$P_n=4[\frac{1-(-1)^n}{\pi^2 n^2}]$ (for all odd n) **(17)**

Rescaling the terms to have the same strength as the forcing amplitude,

$P_n=\frac{P_n}{P_1}\times g$ **(18)**

The forcing term then is;

$f(t)=P_1\cos\omega_1 t+P_3\cos\omega_3 t+P_5\cos\omega_5 t+P_7\cos\omega_7 t$ **(19)**

The present study utilised the popular constant operation time step fourth order Runge-Kutta schemes to simulate equation (1) in the first order rate of equations (2) and (3). The respective details of the scheme are provided in equations **(20)** to **(24)** substituting y for (θ_1,θ_2), x for (t) and constant time step h.

2.5 Fourth-Order Runge-Kutta Scheme

$$y_{i+1} = y_i + \frac{h}{6}[K_1 + 2(K_2 + K_3) + K_4] \quad \textbf{(20)}$$

$$K_1 = f(x_i, y_i) \quad \textbf{(21)}$$

$$K_2 = f\left(x_i + \frac{h}{2}, y_i + \frac{hK_1}{2}\right) \quad \textbf{(22)}$$

$$K_3 = f\left(x_i + \frac{h}{2}, y_i + \frac{hK_2}{2}\right) \quad \textbf{(23)}$$

$$K_4 = f(x_i + h, y_i + hK_3) \quad \textbf{(24)}$$

2.6 Study parameters

2.6.1 Duffing Oscillator

From literature research, this study focuses on the parameters defined by; the non-dimensional forcing amplitude (P_o = 0.168), damping constant (γ = 0.21). Simulation of these parameters was carried out over the drive frequency ω_Dt = 1. The simulation time step is fixed at h= $\frac{T_P}{500}$for $T_P = \frac{2\pi}{\omega_D}$ and the initial condition for the studied cases is (0, 0). The simulation was executed for 2000-excitation periods (i.e. $10T_P - 2010T_P$).

2.6.2 Pendulum Oscillator

From literature research, this study focuses on the parameters defined by; damping qualities,

(q) =4.0, drive amplitude $(g) = 1.5$ and frequency $(\omega_D) = 2/3$. The simulation time step is fixed at h= $\frac{T_P}{500}$for $T_P = \frac{2\pi}{\omega_D}$ and the initial condition for studied cases is (0, 0). The simulation was executed for 2000-excitation periods (i.e. $10T_P - 2010T_P$).

3.0 RESULTS AND DISCUSSION

3.1 Duffing Oscillator

The Poincare patterns in fig. 3 compare excellently well with those reported by [7], amplitude (P_o = 0.168), damping constant (γ = 0.21) fixed drive frequency of 2/3. Fig. 4 and 5 show the Poincare solutions (scatter plots), with attractor layout of periodically excited duffing oscillator using a fractal disk scale of 2. The scatter plots distribution per unit space area varies non-uniformly from one location to another. This shows that nonlinear duffing oscillators under periodic excitations are chaotic.

Tables 1-3 show the variation of optimum counted disks with increasing observation scale number for the referenced harmonic excitation and the periodic excitation simulation periods.

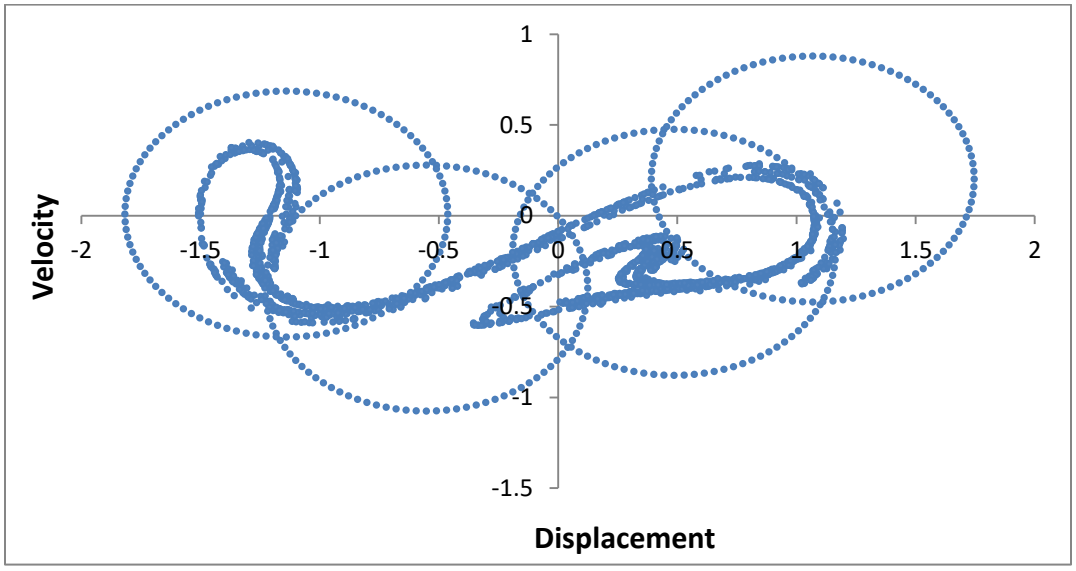

Fig 5. Poincare section of harmonically excited duffing oscillator showing the attractor layout for scale 2 disk.

Table 1. The generated report (10 trials) of disk laying of the Poincare (harmonic excitation)

Scale	Optimum disk count	Trial 1	Trial 2	Trial 3	Trial 4	Trial 5	Trial 6	Trial 7	Trial 8	Trial 9	Trial 10
1	2	2	3	2	2	2	2	2	2	2	2
2	4	6	5	4	5	5	4	4	5	4	5
3	8	9	8	8	9	9	8	8	8	9	8
4	12	12	12	14	12	12	13	15	12	12	12
5	16	17	20	19	18	16	19	17	18	17	18
6	21	23	24	23	21	22	22	23	21	22	23
7	23	28	28	27	23	27	28	27	28	29	26
8	29	32	31	32	33	33	30	33	34	34	29
9	36	36	40	40	39	39	37	40	38	38	38
10	40	41	45	40	44	46	41	41	45	43	44

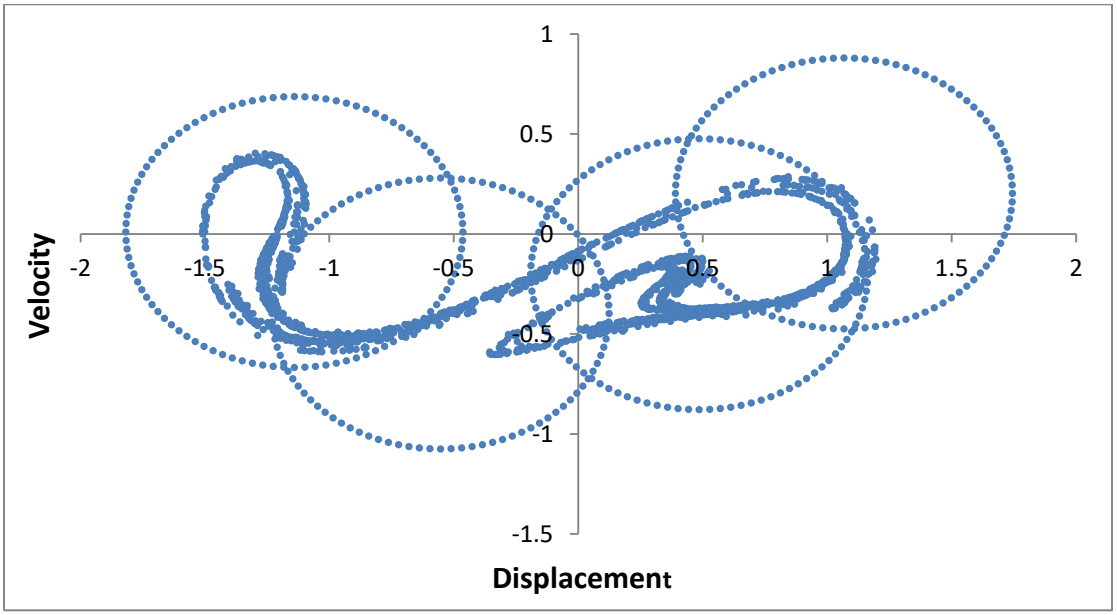

Fig 6. Poincare section of periodically excited duffing (excitation 1) showing the attractor layout for scale 2 disk.

Table 2. The generated report (10 trials) of disk laying of the Poincare (periodic excitation 1)

Scale	Optimum disk count	Trial 1	Trial 2	Trial 3	Trial 4	Trial 5	Trial 6	Trial 7	Trial 8	Trial 9	Trial 10
1	2	2	2	2	2	2	2	2	2	2	2
2	4	5	5	6	5	4	4	6	6	6	5
3	8	9	10	8	9	9	9	9	9	9	9
4	12	13	13	12	12	14	14	15	14	14	14
5	17	18	20	18	19	17	21	20	18	18	18
6	21	23	24	21	24	26	23	22	25	24	25
7	28	31	29	32	29	31	30	33	32	28	32
8	33	39	36	33	35	38	35	34	34	36	35
9	41	43	44	41	43	47	42	45	43	43	44
10	44	45	49	49	46	44	47	50	51	46	51

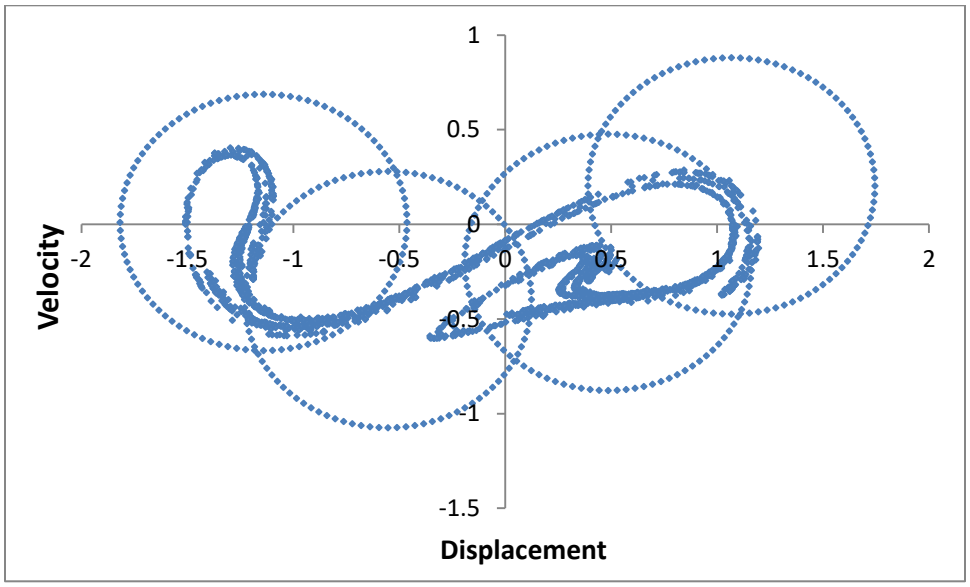

Fig 7. Poincare section of periodically excited duffing (excitation 2) showing the attractor layout for scale 2 disk.

Table 3. The generated report (10 trials) of disk laying of the Poincare (periodic excitation 2)

Scale	Optimum disk count	Trial 1	Trial 2	Trial 3	Trial 4	Trial 5	Trial 6	Trial 7	Trial 8	Trial 9	Trial 10
1	2	3	3	2	3	3	3	3	3	3	2
2	4	5	5	5	6	5	5	5	5	4	4
3	8	10	9	10	9	8	9	9	8	9	9
4	13	15	14	14	14	14	14	13	13	14	13
5	16	17	17	16	18	16	18	16	17	18	16
6	20	21	21	20	23	22	22	22	21	21	21
7	25	27	25	26	26	26	27	25	26	26	26
8	29	31	31	30	30	31	30	29	29	31	31
9	34	35	35	38	36	37	36	37	34	39	34
10	37	44	37	43	38	40	40	40	42	42	44

Table 4. Disk count and Logarithm of disk count

	Disks Counted			Natural Logarithms			
Observation Scales	**Harmonic Excitation**	**Periodic Excitation 1**	**Periodic Excitation 2**	**Observation Scales**	**Harmonic Excitation**	**Periodic Excitation 1**	**Periodic Excitation 2**
1	2	2	2	0.00	0.69	0.69	0.69
2	4	4	4	0.69	1.39	1.39	1.39
3	8	8	8	1.10	2.08	2.08	2.08
4	12	12	13	1.39	2.48	2.48	2.56
5	16	17	16	1.61	2.77	2.83	2.77
6	21	21	20	1.79	3.04	3.04	3.00
7	23	28	25	1.95	3.14	3.33	3.22
8	29	33	29	2.08	3.37	3.50	3.37
9	36	41	34	2.20	3.58	3.71	3.53
10	40	44	37	2.30	3.69	3.78	3.61

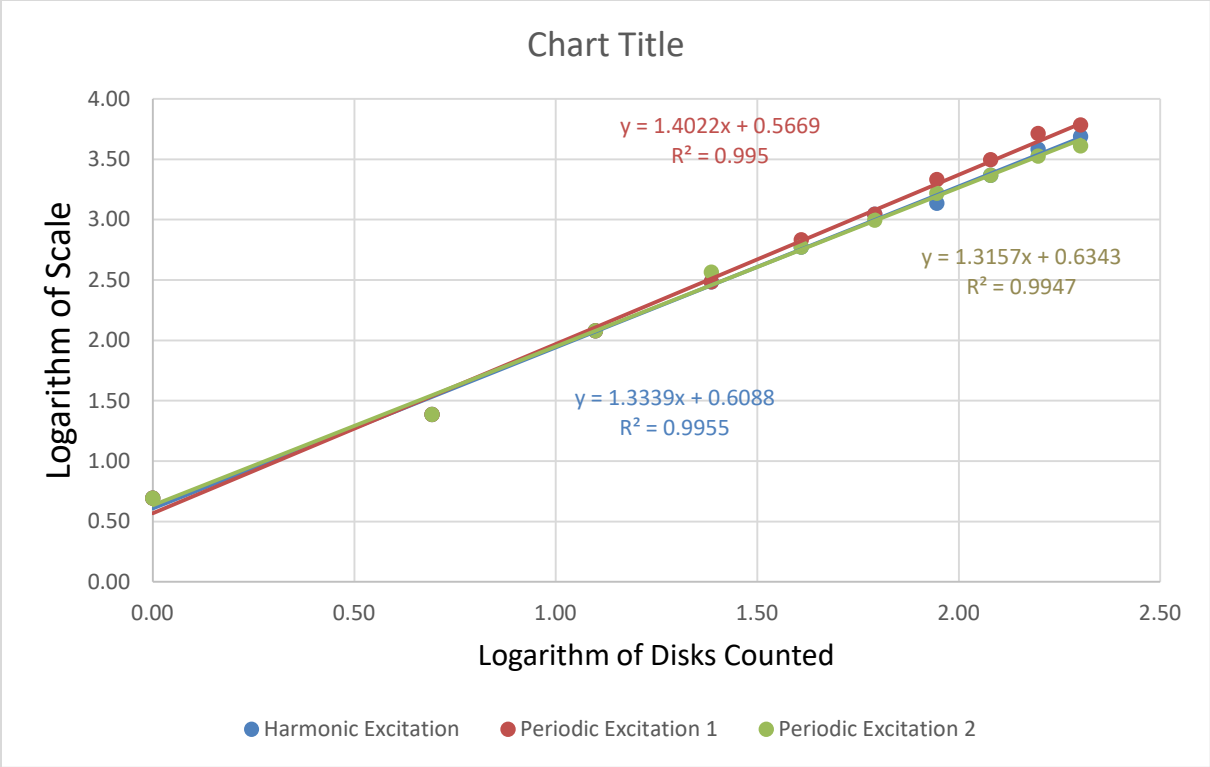

Fig 8. Log=Log plots of disks required for the overlay

Table 4 shows a sample of optimum variation of disks counted for ten (10) different observations scale for the three (3) investigated cases. The slope of line of best fit in figure 8 is an expression of the fractal quantification of space filling ability of the Poincare given in fig. 5, 6 and 7.

Fig. 7 (triangular wave form excitation) with estimated fractal disk dimension values of 1.315, coefficient of fitness (R^2=0.994) is quite similar quantitatively to that of the harmonic excitation (fig. 5) which has an estimated dimension value of 1.333 and a coefficient of fitness (R^2=0.995). It can be argued that the Poincare produced by the square wave form periodic excitation fill space more than both the Poincare produced by the harmonic and the triangular wave form. Its estimated fractal disk dimension value is 1.2553 with coefficient of fitness (R^2=0.997).

3.2 Pendulum Oscillator

The Poincare patterns in fig. 9 compare excellently well with those reported by [19] for damp quality 4, fixed excitation amplitude of 1.5 and fixed drive frequency of 2/3. Fig. 10 and 11 show the Poincare solutions (scatter plots), with attractor layout of periodically excited pendulum using a fractal disk scale of 2. The scatter plots distribution per unit space area varies non-uniformly from one location to another. This shows that nonlinear pendulums under periodic excitations are chaotic.

Tables 5-7 show the variation of optimum counted disks with increasing observation scale number for the referenced harmonic excitation and the periodic excitation simulation periods.

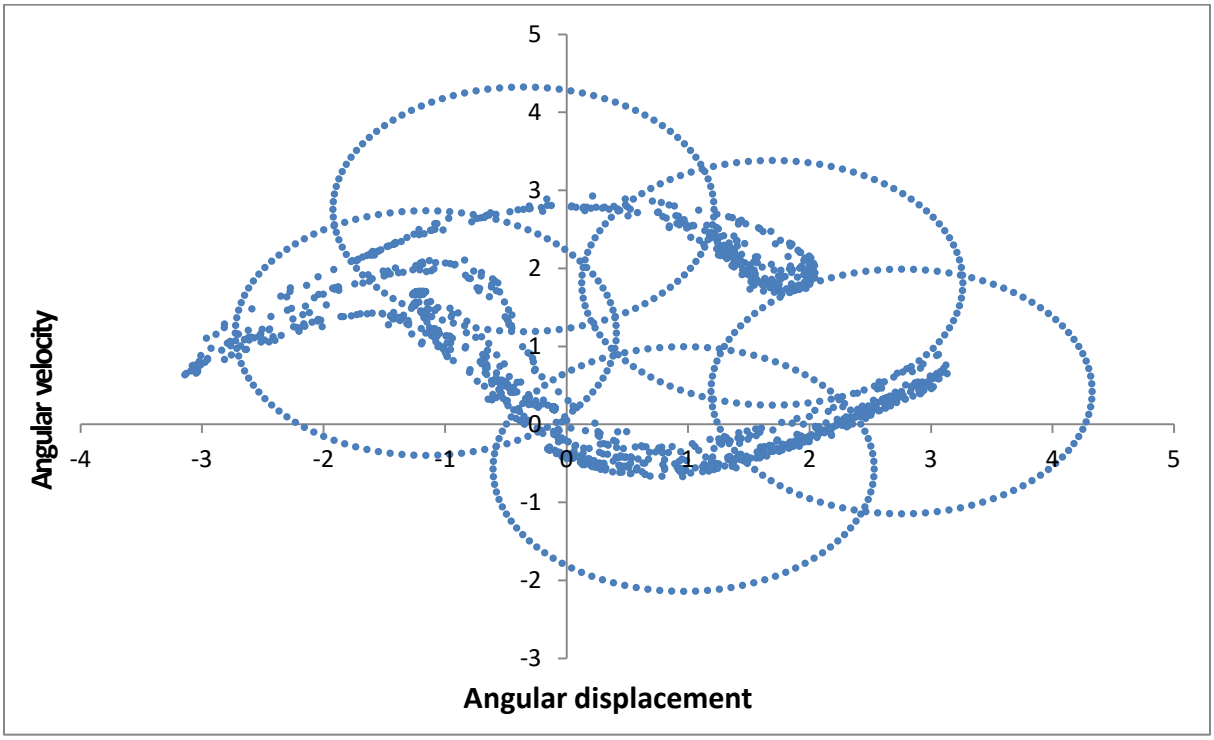

Fig 9. Poincare section of harmonically excited pendulum showing the attractor layout for scale 2 disk

Table 5. The generated report (10 trials) of disk laying of the Poincare (harmonic excitation)

Scale	Optimum disk count	Trial 1	Trial 2	Trial 3	Trial 4	Trial 5	Trial 6	Trial 7	Trial 8	Trial 9	Trial 10
1	2	2	2	3	2	3	3	2	2	2	3
2	5	6	6	6	5	6	7	6	6	6	6
3	9	9	9	10	10	9	9	9	9	9	9
4	12	14	12	13	12	12	13	13	12	12	12
5	15	16	17	16	16	17	16	16	15	15	17
6	18	20	22	20	18	20	20	21	19	21	20
7	23	24	24	23	26	23	25	24	23	26	23
8	28	29	28	30	30	30	29	28	30	31	28
9	33	37	34	36	33	35	35	37	34	36	36
10	39	39	41	40	40	43	40	40	40	42	40

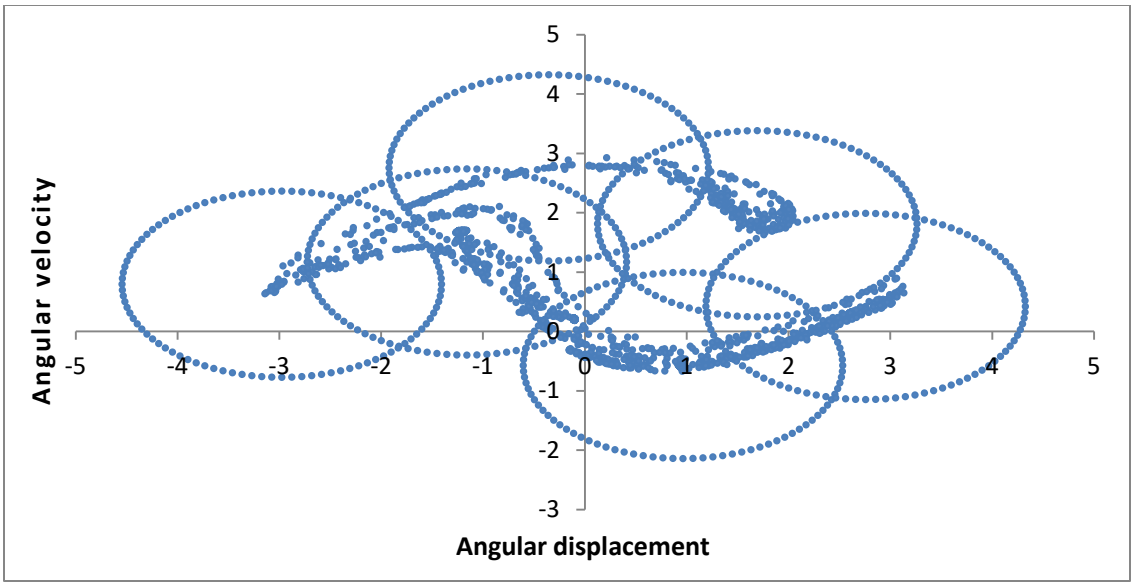

Fig 10. Poincare section of periodically excited pendulum (excitation 1) showing the attractor layout for scale 2 disk

Table 6. The generated report (10 trials) of disk laying of the Poincare (periodic excitation 1)

Scale	Optimum disk count	Trial 1	Trial 2	Trial 3	Trial 4	Trial 5	Trial 6	Trial 7	Trial 8	Trial 9	Trial 10
1	2	3	2	2	2	2	3	3	2	3	2
2	6	6	7	6	6	6	6	6	6	7	6
3	8	10	10	10	9	9	9	8	9	10	9
4	12	14	13	14	13	14	13	15	14	12	13
5	17	17	19	19	19	19	18	18	17	19	18
6	20	20	25	24	26	24	23	26	26	23	23
7	28	30	32	30	33	30	29	30	31	30	28
8	35	36	35	38	39	36	36	38	37	36	40
9	41	44	45	43	47	46	44	41	49	41	47
10	49	52	52	55	51	50	50	51	49	51	54

Scale	Optimum disk count	Trial 1	Trial 2	Trial 3	Trial 4	Trial 5	Trial 6	Trial 7	Trial 8	Trial 9	Trial 10
1	2	2	2	3	2	2	2	3	3	2	2
2	6	6	7	6	6	7	7	6	6	7	7
3	8	9	11	8	8	9	8	9	9	9	10

Table 7. The generated report (10 trials) of disk laying of the Poincare (periodic excitation 2)

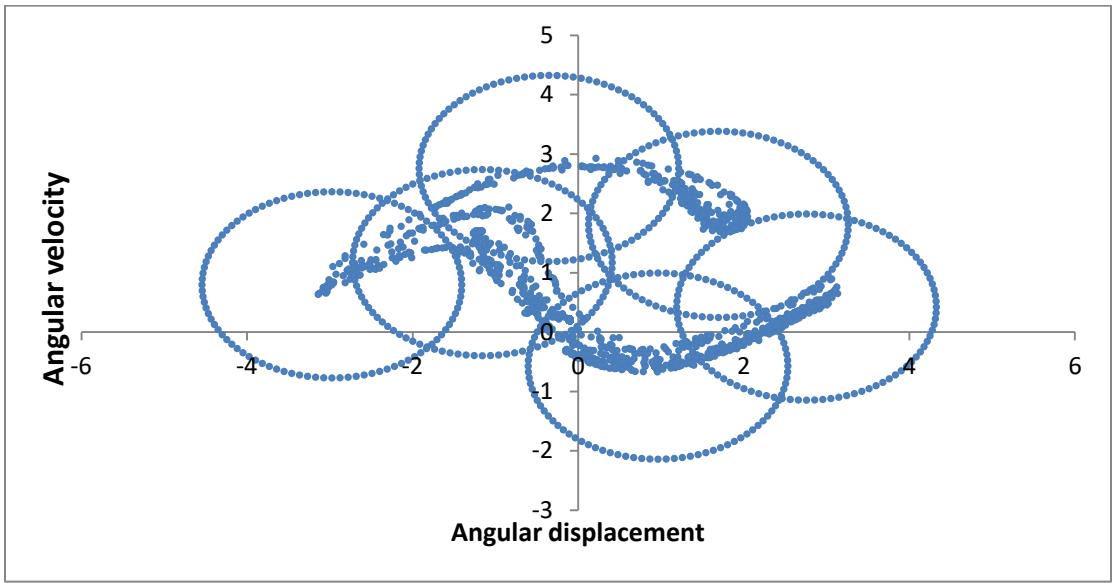

Fig 11. Poincare section of periodically excited pendulum (excitation 2) showing the attractor layout for scale 2 disk.

4	12	14	12	13	12	12	14	12	12	14	14
5	17	18	18	19	18	18	18	17	20	18	19
6	21	22	21	22	25	23	23	21	23	23	24
7	26	29	27	29	29	26	28	27	28	27	30
8	32	34	37	35	32	32	38	35	36	37	36
9	39	42	39	41	41	42	41	39	43	46	45
10	48	52	55	50	49	51	53	50	51	49	48

Table 8. Disk count and Logarithm of disk count

	DISKS COUNTED			NATURAL LOGARITHMS			
Observation Scales	**Harmonic Excitation**	**Periodic Excitation 1**	**Periodic Excitation 2**	**Observation Scales**	**Harmonic Excitation**	**Periodic Excitation 1**	**Periodic Excitation 2**
1	2	2	2	0.00	0.69	0.69	0.69
2	5	6	6	0.69	1.61	1.79	1.79
3	9	8	8	1.10	2.20	2.08	2.08
4	12	12	12	1.39	2.48	2.48	2.48
5	15	17	17	1.61	2.71	2.83	2.83
6	18	20	21	1.79	2.89	3.00	3.04
7	23	28	26	1.95	3.14	3.33	3.26
8	28	35	32	2.08	3.33	3.56	3.47
9	33	41	39	2.20	3.50	3.71	3.66
10	39	49	48	2.30	3.66	3.89	3.87

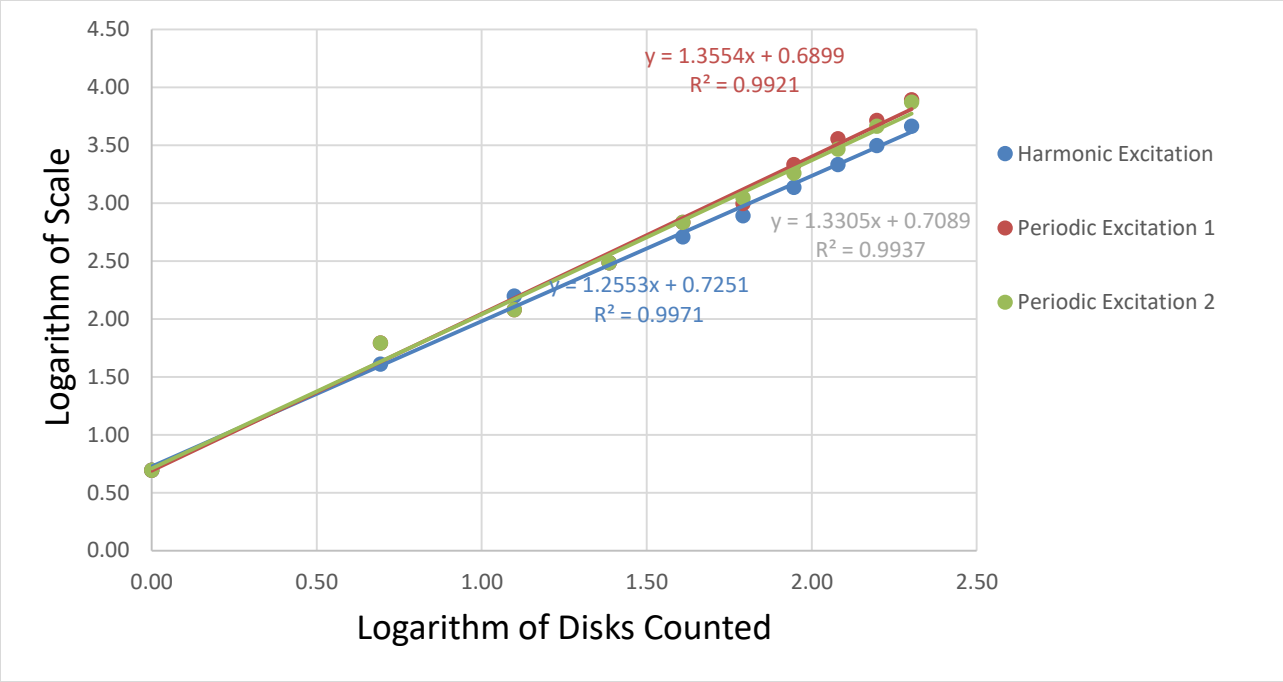

Fig 12. Log plots of disks required for the overlay

Table 8 shows a sample of optimum variation of disks counted for ten (10) different observations scale for the three (3) investigated cases. The slope of line of best fit in figure 12 is an expression of the fractal quantification of space filling ability of the Poincare given in figures 9, 10 and 11.

Therefore, it can be argued that figures 10 and 11 with estimated fractal disk dimension values of 1.3554, coefficient of fitness (R^2=0.9921) and 1.3305, coefficient of fitness (R^2=0.993) respectively, fill space more than figure 9 with estimated fractal disk dimension value of 1.2553 with coefficient of fitness (R^2=0.997).

4.0 CONCLUSIONS

Qualitatively, the effect of periodic excitation on the duffing system is the same as that of the harmonic excitation on it. However, the number of disks required to cover the Poincare varied from harmonic to periodic excitations. This implies that the effects are quite different quantitatively. Under the harmonic excitation, the Poincare has a dimension of 1.333 and under the selected periodic excitations, the fractal dimensions are 1.402 and 1.315. This implies that the Poincare of the periodically excited duffing (square waveform) occupied more space on the 2D-euclidean space than that of the harmonically excited duffing. The absolute variation in dimension is between 4.92% and 1.37%.

Qualitatively, the effect of periodic excitation on the pendulum system is the same as that of the harmonic excitation on it. However, the number of disks required to cover the Poincare varied from harmonic to periodic excitations. This implies that the effects are quite different quantitatively. Under the harmonic excitation, the Poincare has a dimension of 1.2553 and under the selected periodic excitations, the fractal dimensions are 1.3554 and 1.3305. This implies that the Poincare of the periodically excited pendulum occupied more space on the 2D-euclidean space than that of the harmonically excited pendulum. The

variation in dimension is between 5.67% and 7.39%. Therefore, the effect of periodic excitations on dynamic systems should also be of interest as there is a relatively large difference.

REFERENCES

1. Cuairan, M. T., Gieseler, J., Meyer, N., & Quidant, R. Precision Caliberation of the Duffing Oscillator with Phase Control. 2021, 1: 1-6
2. Sekar, P., & Narayaran, S. Chaos in Mechanical Systems – A Review. 1995, 20: 529-582
3. Dooren, R. Van. Behaviour in the Duffing Oscillator. 1988, 123: 327-339.
4. Ramadoss, J., Kengne, J., Tsamene, S., Rajagopal, K., & Djuidje, G. (2022). Chaos , Solitons and Fractals Reversal of Period doubling , Multistability and Symmetry Breaking Aspects for a System Composed of a van der pol Oscillator Coupled to a Duffing Oscillator. *Chaos, Solitons and Fractals. 2022.* https://doi.org/10.1016/j.chaos.2022.112157
5. Jauregui, J. C. (2014). NonLinear Vibration In *Parameter* Identification and Monitoring of *Mechanical Systems under Nonlinear Vibration. 1st ed. Mexico: Woodhead Publishing;2014* (35–53).
6. Han, N., & Li, Z. The Oscillating Periodic Solutions of a Classical Pendulum System with Smooth and Discontinuous Dynamics. *European Physical Journal Plus*. 2021, *136*(3). https://doi.org/10.1140/epjp/s13360-021-01240-2
7. Salau, T. A. ., & Ajide, O. Comparative Analysis of Time Steps Distribution in Runge Kutta Algorithm. International Journal of Scientific and Engineering *Research*. 2012, *3*(1): 1–5.
8. El-Tantawy, S. A., Salas, A. H., & Alharthi, M. R. On the Analytical Solutions of the Forced Damping Duffing Equation in the Form of Weierstrass Elliptic Function and its Applications. *Mathematical Problems in Engineering*, *2021*. https://doi.org/10.1155/2021/6678102.
9. Zufiria, P. J., & Jiménez, S. *Characterizing chaos in a type of fractional Duffing's Equation*. 2015, 660–669. https://doi.org/10.3934/proc.2015.0660.
10. Han, Ning, and Qingjie Cao. Rotating Pendulum with Smooth and Discontinuous Dynamics. International Journal of Mechanical Sciences. 2016, 127:91-102.
11. Özer, A.B. and Akin, E., (2005). *Tools for detecting chaos*, Journal of SAÜ Institute of science and technology, 9(1), p.60-66.
12. Chau, K.T and Zheng, W. Chaos in Electric Drive Systems: Analysis, Control and Application. 2011, John Wiley & Sons. Ltd. ISBN 978-0-470-82633-1, pp. 4.
13. Wawrzynski, W. Duffing-Type Oscillator Under Harmonic Excitation with a Variable Value of Excitation Amplitude and Time-Dependent External Disturbances. 2021, *Scientific Reports*, *11*(1):1–15. https://doi.org/10.1038/s41598-021-82652.
14. Mandelbrot, B.B. The Fractal Geometry of Nature. 1982, W.H. Freeman ansd Co. New York, ISBN 0-7167-1186-9

15. Salau T. A.O. and Ajide O.O. A Novel Graphic Presentation and Fractal characterization of Poincare Solution of Harmonically Excited Pendulum. International Journal of Advances in Engineering & Technology. 2013, 6(3): 1299-1312.

16. Savi, M. A. Nonlinear Dynamics and Chaos Nonlinear Dynamics and Chaos. 2017, https://doi.org/10.1007/978-3-319-29982-2.

17. Jacobo, A., Ricardo, L.V. and Miguel, A.F.S. Fractal Structures in Nonlinear Dynamics. American Physical Society's New Journal.2009, 81(1): 333-386.

18. Guckenheimer J., Holmes P. Nonlinear Oscillations, Dynamical Systems and Bifurcations of Vector Fields. Springer-Verlag, New York, 1983.

19. Gregory, L.B. and Jerry, P. J. Chaotic Dynamics: An introduction. 1990, Cambridge University Press, New York, ISBN 0-521-38258-0 Hardback, ISBN 0-521-38897-X.